Conformational Analysis and Intramolecular Interactions of L-Proline Methyl Ester and Its N-Acetylated Derivative through Spectroscopic and Theoretical Studies

ARTICLE *in* THE JOURNAL OF PHYSICAL CHEMISTRY A · FEBRUARY 2014

Impact Factor: 2.69 · DOI: 10.1021/jp5007632 · Source: PubMed

THE JOURNAL OF PHYSICAL CHEMISTRY A

Article

pubs.acs.org/JPCA

Conformational Analysis and Intramolecular Interactions of L-Proline Methyl Ester and Its *N*-Acetylated Derivative through Spectroscopic and Theoretical Studies

Carolyne B. Braga,[†] Lucas C. Ducati,[‡] Cláudio F. Tormena,[†] and Roberto Rittner*[,†]

[†]Physical Organic Chemistry Laboratory, Chemistry Institute, University of Campinas, 13083-970 Campinas, SP, Brazil

[‡]Chemistry Institute, University of Sao Paulo, 05513-970 São Paulo, SP, Brazil

Supporting Information

ABSTRACT: This work reports a detailed study regarding the conformational preferences of L-proline methyl ester (ProOMe) and its *N*-acetylated derivative (AcProOMe) to elucidate the effects that rule their behaviors, through nuclear magnetic resonance (NMR) and infrared (IR) spectroscopies combined with theoretical calculations. These compounds do not present a zwitterionic form in solution, simulating properly amino acid residues in biological media, in a way closer than amino acids in the gas phase. Experimental $^3J_{HH}$ coupling constants and infrared data showed excellent agreement with theoretical calculations, indicating no variations in conformer populations on changing solvents. Natural bond orbital (NBO) results showed that hyperconjugative interactions are responsible for the higher stability of the most populated conformer of ProOMe, whereas for AcProOMe both hyperconjugative and steric effects rule its conformational equilibrium.

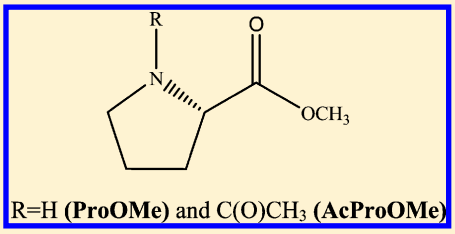

R=H **(ProOMe)** and C(O)CH$_3$ **(AcProOMe)**

1. INTRODUCTION

A full knowledge of the conformational equilibria of proteinogenic amino acids and their intramolecular interactions is a fundamental step toward the understanding of three-dimensional structures of peptides and proteins. Thus, amino acids have been the object of many investigations to determine and analyze their stable conformers. Furthermore, they are an attractive target for theoretical and spectroscopic studies due to their conformational flexibilities and the presence of intramolecular interactions.[1−3] However, several limitations regarding their studies have been reported, concerning the complexity of obtaining both theoretical and experimental information. The problem of working with amino acids in solution is mostly due to the fact that these compounds are stabilized as zwitterions ($^+NH_3-CHR-COO^-$) by a network of intermolecular hydrogen bonds, which do not occur in the environment of an amino acid residue in a polypeptide chain or protein.[4,5] Moreover, these ionic forms are also poorly soluble in organic solvents, resulting in an additional barrier to their studies, including nuclear magnetic resonance (NMR) spectroscopy, one of the most powerful tools for structural elucidation.

An alternative that has been applied is the study of amino acids in gas phase, mainly by rotational spectroscopies,[2,6−11] because under these conditions they exhibit an unsolvated neutral form ($NH_2-CHR-COOH$). However, it is difficult to vaporize most amino acids since they are solids with high melting points, low vapor pressures, and present low thermal stability. Despite significant instrumental advances to vaporize amino acids, it is still difficult to extract experimental information on the exact nature of the conformations of these molecules and their quantitative distributions. Furthermore, their extraordinary conformational flexibilities, which result in an unusually large number of low energy conformers, generate difficulties not only for experimental methods but also for theoretical calculations.

An approach, proposed by our group, to supersede the experimental problems mentioned above is to analyze the esterified and *N*-acetylated derivatives of amino acids.[12,13] These compounds do not exist as zwitterions in solution and are soluble in a majority of organic solvents, making possible their studies in solution by properly simulating the amino acid residues in biological media, better than amino acids in the gas phase.

The structural properties of L-proline, one of 20 natural amino acids, has attracted considerable interest over the years due to its distinctive cyclic structure. Its nitrogen atom is covalently bonded to the side chain and forms a pyrrolidine ring, giving L-proline considerable conformational rigidity compared to other amino acids. The flexibility of this five-membered ring adds new structural characteristics, which make its chemistry quite interesting and unique. Because of these conformational properties, L-proline plays many important biological roles, including determination of the β-turn structure in polypeptides and proteins, especially in collagen.[14]

A large number of studies have reported the most stable conformations of L-proline and their relative energies.[2,15−18] A detailed discussion of vicinal proton−proton coupling constants and the pseudorotation properties of the pyrroline ring was performed by Haasnoot et al.,[16] which relates the dihedral angle and *J* values with the Karplus relationship, including a correction

Received: January 22, 2014
Revised: February 14, 2014
Published: February 17, 2014

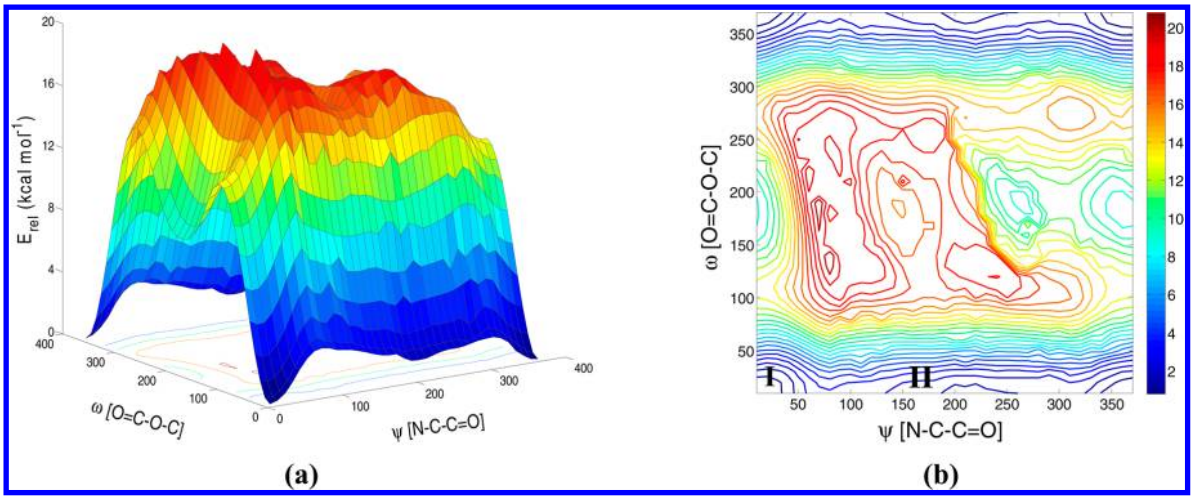

Figure 1. (a) Three-dimensional potential energy surface built by rotating the ψ[N−C−C═O] and ω[O═C−O−C] dihedral angles of ProOMe, at the B3LYP/cc-pVDZ level of theory. (b) Contour map as a function of the ψ and ω dihedral angles. Structures for **I** and **II** are shown in Figure 3.

for the effects of substituent electronegativities, in an empirical way. Moreover, theoretical calculations using density functional theory (DFT) method combined with NMR data for L-proline and *N*-acetyl-L-proline[17] has given two and four conformers, respectively, while in a more recent paper[18] the calculations were performed at MP2 theoretical level and variable temperature NMR experiments to investigate rotational energy barriers, giving similar results to the previous study. However, the only explanation proposed for the interactions that stabilize the conformations is based on the presence of intramolecular hydrogen bonding (IHB). In contrast, results obtained by our group have shown that IHB is not the only source of stability for amino acids and their derivatives but, more importantly, a combination of steric and hyperconjugative effects.[12,13,19−21]

Thus, the present work reports the study of the conformational analysis of L-proline methyl ester (ProOMe) and *N*-acetyl-L-proline methyl ester (AcProOMe) and describes the intramolecular interactions involved in the most stable conformers. To this end, theoretical calculations and NMR and infrared (IR) spectroscopies were employed. The experimental data are supported by DFT calculations, in conjunction with natural bond orbital (NBO) and quantum theory of atoms in molecules (QTAIM) analyses.

2. EXPERIMENTAL AND COMPUTATIONAL DETAILS

2.1. Synthesis of the Compounds. *2.1.1. L-Proline Methyl Ester.* ProOMe was prepared by the deprotonation of its respective salt using activated zinc dust, according the following procedure.[22] L-Proline methyl ester hydrochloride (165.6 mg, 1.0 mmol), commercially available, was mixed with 10.0 mL of dichloromethane in a 25.0 mL round-bottom flask. To this suspension activated zinc dust (100 mg) was added in one portion. The mixture was stirred for 3 h at room temperature until complete deprotonation was achieved, then it was filtered and concentrated in vacuo. The free amino ester was obtained as a light yellow crystalline solid (118.0 mg, 0.9 mmol, 91.4% yield). IR (KBr): ν = 3449 (s), 2957 (w), 2895 (w), 1736 (s), 1447 (m), 1236 (m) cm^{-1}. ^{1}H NMR (600.17 MHz, DMSO-d_6, 25 °C, TMS): δ (ppm) = 3.78 ppm (dd, ^3J = 8.7 and 6.0 Hz, 1H), 3.66 ppm (s, 3H), 2.99 ppm (m, 1H), 2.84 ppm (m, 1H), 2.06 ppm (m, 1H), 1.75 ppm (m, 1H), 1.70 ppm (m, 2H). ^{13}C NMR (150.91 MHz, DMSO-d_6, 25 °C, TMS): δ (ppm) = 174.12, 59.67, 52.59, 47.28, 29.65, 25.06. MS (EI+): calcd for $C_6H_{11}NO_2$, 129.0790; found 129.0793 $[M]^+$.

2.1.2. N-Acetyl-L-proline Methyl Ester. AcProOMe was prepared by the esterification of *N*-acetyl-L-proline.[23,24] To 10.0 mL of methanol at −5 °C, 0.5 mL (6.4 mmol) of thionyl chloride was added dropwise with stirring. After the solution had been maintained at −5 °C over a period of 10 min, 1.0 g (6.4 mmol) of *N*-acetyl-L-proline (commercially available) was added in portions, and the solution was stirred at this temperature for 3 h. Next, the mixture was allowed to warm to room temperature and stirred further for 24 h. After the methanol had been evaporated, the residue was dissolved in 5 mL of water, and 5 mL of dichloromethane was added. A saturated solution of potassium bicarbonate was added until pH 7 was reached. The organic layer was separated by decantation, and the resulting solution was extracted with successive portions of dichloromethane. The combined extracts were dried over anhydrous magnesium sulfate, and the solvent was removed on a rotary evaporator, resulting in 684.5 mg (3.3 mmol, 51.5% yield) of *N*-acetyl-L-proline methyl ester hydrochloride. To this compound in chloroform solution (5.0 mL), 0.4 mL of triethylamine was added dropwise with stirring, which was maintained for 4 h. The mixture was heated at 70 °C for 1 h, then cooled to room temperature and concentrated in vacuo. The oily liquid was mixed with 10 mL of water and 10 mL of a saturated solution of sodium bicarbonate and extracted with dichloromethane. The collected organic layers were dried over anhydrous sodium sulfate. This solution was concentrated under reduced pressure to yield 484.4 mg (2.8 mmol, 85.8% yield) of *N*-acetyl-L-proline methyl ester as a colorless liquid. IR (NaCl): ν = 2978 (m), 2955 (m), 2880 (m), 1747 (s), 1654 (s), 1435 (s), 1418 (s), 1200 (m), 1175 (m) cm^{-1}. ^{1}H NMR (600.17 MHz, DMSO-d_6, 25 °C, TMS): cis rotamer, δ (ppm) = 4.61 (dd, ^3J = 8.7 and 2.6 Hz, 1H), 3.69 (s, 3H), 3.36 (m, 2H), 2.23 (m, 1H), 2.05 (m, 1H), 1.86 (m, 1H), 1.84 (s, 3H), 1.72 (m, 1H); trans rotamer, δ (ppm) = 4.25 (dd, ^3J = 8.7 and 4.3 Hz, 1H), 3.60 (s, 3H), 3.52 (m, 2H), 2.15 (m, 1H), 1.97 (s, 3H), 1.91 (m, 2 H), 1.83 (m, 1 H). ^{13}C NMR (150.91 MHz, DMSO-d_6, 25 °C, TMS): cis rotamer, δ (ppm) = 173.26, 168.97, 59.69, 52.80, 46.25, 31.24, 22.84, 22.47; trans rotamer, δ (ppm) = 173.04, 168.81, 58.49, 52.17, 47.69, 29.48, 24.87, 22.49. MS (EI+): calcd for $C_8H_{13}NO_3$, 171.0895; found 171.0897 $[M]^+$.

dx.doi.org/10.1021/jp5007632 | J. Phys. Chem. A 2014, 118, 1748−1758

2.2. NMR Experiments. ^{1}H NMR spectra were recorded on a Bruker Avance III spectrometer operating at 600 MHz for ^{1}H. Spectra were obtained for solutions of ca. 15 mg in 0.7 mL of different solvents (varying from C_6D_6 to DMSO-d_6, according to the solubility of the compound) with a probe temperature of 25 °C, referenced to internal TMS. Typical conditions for ^{1}H spectra were 16 transients, spectral width around 6.0 kHz, and 64 K data points with an acquisition time of ca. 5 s. The free induction decays (FID)s were zero-filled to 128 K giving a digital resolution of 0.09 Hz/point.

2.3. IR Experiments. The IR spectra were recorded on a Shimadzu FT-IR Prestige 21 spectrometer, with 1.0 cm^{-1} resolution, 64 scans, at a concentration of 3.0×10^{-2} mol L^{-1} in carbon tetrachloride, chloroform, dichloromethane, and acetonitrile solutions, using a sodium chloride cell with an optical path of 0.5 mm for the carbonyl region (1800−1600 cm^{-1}). The overlapped carbonyl bands (in the fundamental region) were deconvoluted by means of the GRAMS curve fitting software.[25] The populations of the different conformers were estimated from the maximum of each component of the resolved carbonyl doublet expressed in percentage of absorbance, assuming equal molar absorptivity coefficients for the studied compounds.

2.4. Theoretical Calculations. Potential energy surface (3D PES, Figure 1) was built for ProOMe by simultaneous scanning the ψ[N−C−C═O] and ω[O═C−O−C] dihedral angles from 0° to 360°, in steps of 10°, at the B3LYP/cc-pVDZ level. These dihedral angles are shown in Figure 2a. The resulting energy minima were fully reoptimized, and the frequencies calculated with zero-point energy (ZPE) corrections, at the MP2/aug-cc-pVTZ and ωB97X-D/aug-cc-pVTZ levels of theory.[26]

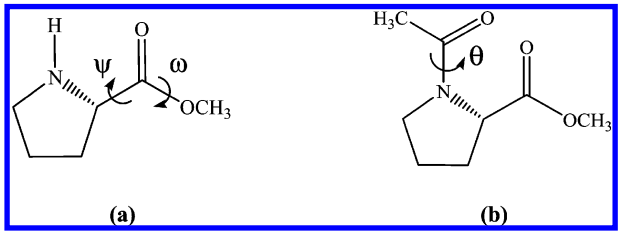

Figure 2. Investigated dihedral angles: (a) ψ and ω of ProOMe and (b) θ of AcProOMe, which provided the corresponding lowest energy conformers.

The lowest energy geometries found for the ProOMe were used as starting points to determine the AcProOMe conformers. From each previously optimized ProOMe main chain geometry, a potential energy curve was obtained by rotating the θ[C−C(═O)−N−C] dihedral angle (Figure 2b), in steps of 10° from 0° to 360°, at the B3LYP/cc-pVDZ level. Then, the conformer energy minima were reoptimized at the ωB97X-D/aug-cc-pVTZ level, and their frequencies were calculated with ZPE corrections.

Subsequently, the IEF-PCM (integral equation formalism polarizable continuum model)[27] was used for geometry optimization calculations to evaluate solvent effects on the relative stability of the most stable conformers of the compounds in solvents of different dielectric constants. The $^3J_{HH}$ vicinal spin−spin coupling constants were calculated for each conformer in solution using the IEF-PCM model at the B3LYP/EPR-III level for hydrogen atoms. All the calculations were performed using the Gaussian09 program package.[28]

Finally, interpretation of the conformer stabilities was provided by means of NBO analysis and by QTAIM, at the ωB97X-D/aug-cc-pVTZ level, using the structures optimized in isolated phase. NBO calculations were performed through module NBO 5.0 of the Gaussian09 program,[29] while the QTAIM was carried out with the AIMALL software.[30]

3. RESULTS AND DISCUSSION

Initially, theoretical calculations were carried out in isolated phase, and the stable conformers of ProOMe were identified by analyzing the 3D PES and the corresponding contour map, presented in Figure 1. The two minima that appear in the PES (**I** and **II**, Figure 3) were optimized without symmetry restrictions using both ωB97X-D and MP2/aug-cc-pVTZ levels of theory, in such a way that reliable values of energies and structural parameters were achieved. Although MP2 is probably the best choice to obtain accurate conformational energies, it has the drawback of being very expensive for vibrational frequencies. Thus, since the ωB97X-D functional showed good agreement with the obtained values by MP2 (Table 1), the ωB97X-D method was used for further calculations. This functional was chosen because it includes empirical atom−atom dispersion corrections and provides significant improvement for noncovalent interactions compared to the other previous functionals such as ωB97X.

Calculated energies demonstrate that the conformer **I** is 1.29 kcal mol^{-1} (at ωB97X-D) more stable than conformer **II**. It was verified that the main difference between these conformations is related to the pyrrolidine ring flexibility, where in **I** the ψ dihedral angle [N−C−C═O ≈ 6°] presents a cis arrangement, and the backbone atoms [C−O−C(O)−C−N] are nearly coplanar; whereas in **II** the nitrogen atom suffers a deviation from

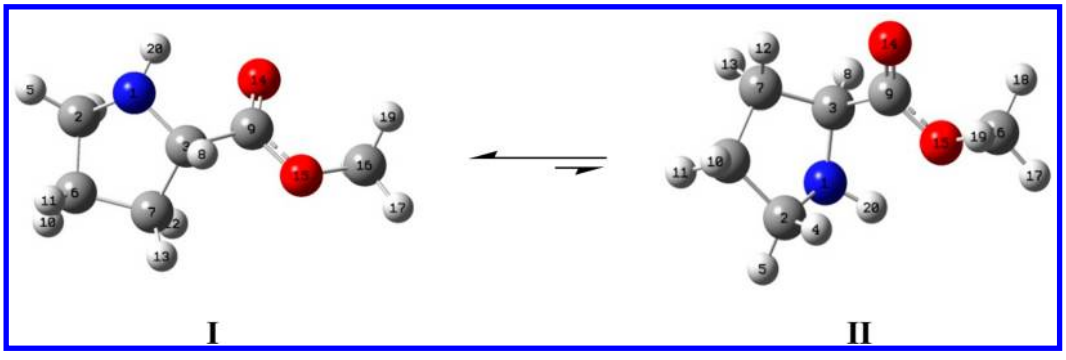

Figure 3. Most stable conformers of ProOMe, cis (**I**) and trans (**II**) (defined by the N−C−C═O dihedral angle), obtained at the ωB97X-D/aug-cc-pVTZ level of theory.

dx.doi.org/10.1021/jp5007632 | J. Phys. Chem. A 2014, 118, 1748−1758

Table 1. Calculated Structural Parameters,[a] Energies (E),[b] and Dipole Moments (μ) for the Optimized Conformer Structures of ProOMe in Isolated Phase, at the ωB97X-D/aug-cc-pVTZ Level of Theory; the Values Obtained from MP2/aug-cc-pVTZ Level Are in Parentheses

parameter	I	II
$r(N_1-H)$	1.010 (1.015)	1.009 (1.014)
$r(N-C_3)$	1.456 (1.463)	1.450 (1.457)
$r(C_3-C_9)$	1.517 (1.512)	1.533 (1.529)
$r(NH\cdots O_{14})$	2.359 (2.347)	
$r(NH\cdots O_{15})$		2.374 (2.322)
$\angle NH\cdots O_{14}$	105.3 (106.2)	
$\angle NH\cdots O_{15}$		99.6 (101.6)
ω[O=C−O−C]	1.2 (0.7)	0.5 (0.0)
ψ[N−C−C=O]	6.2 (7.5)	154.7 (151.7)
E (au)	−440.31677 (−439.48949)	−440.31472 (−439.48752)
E_{rel} (kcal mol^{-1})[c]	0.00 (0.00)	1.29 (1.24)
μ (debye)	2.05 (2.10)	1.89 (1.83)
population (%)	89.8 (89.0)	10.2 (11.0)

[a]Bond lengths in angstroms (Å); bond and dihedral angles in degrees. [b]ZPE correction included. [c]1 au = 627.5095 kcal mol^{-1}.

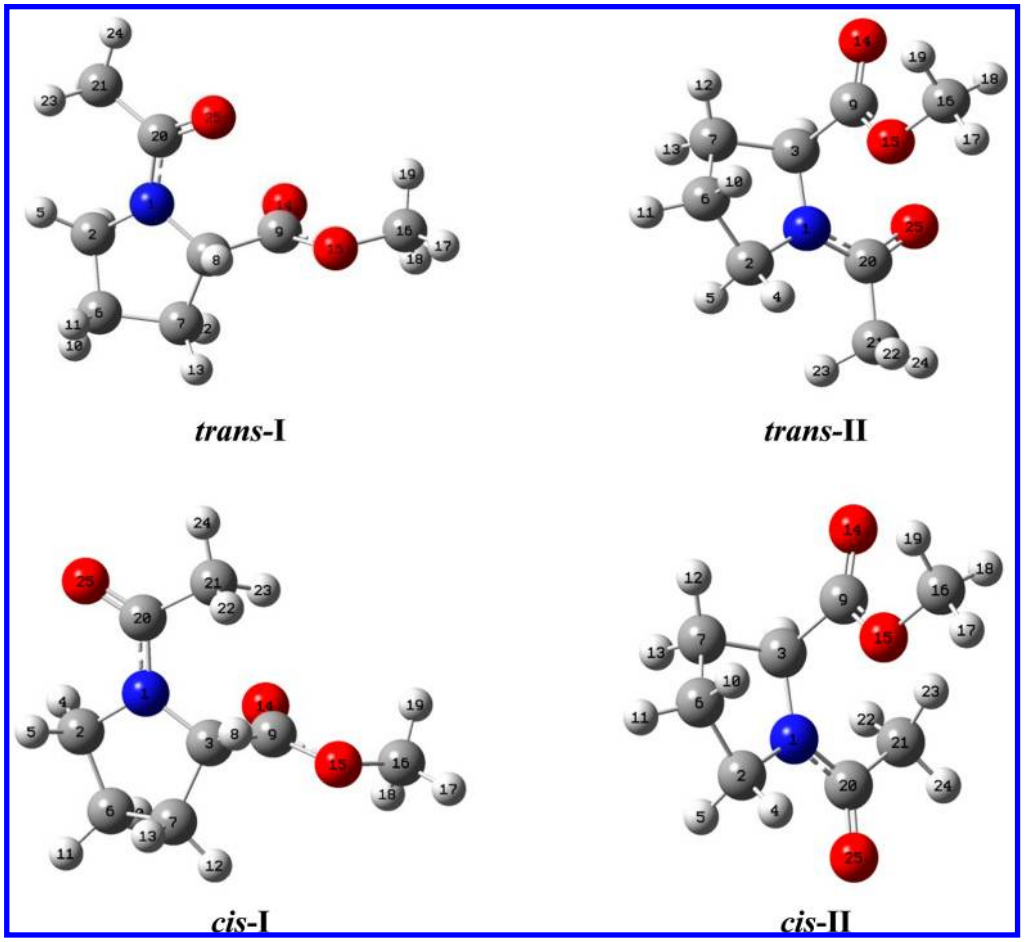

Figure 4. Most stable conformers of AcProOMe obtained at the ωB97X-D/aug-cc-pVTZ level of theory.

backbone planarity, and the ψ dihedral angle [N−C−C=O ≈ 155°] is in a trans disposition.

In turn, each **I** and **II** form presented two rotamers (cis and trans) due to rotation about the *N*-COMe bond for AcProOMe, resulting in the four conformers illustrated in Figure 4. The cis−trans nomenclature was based in previous studies,[31] which related the amide methyl group to the C(O)−OCH$_3$.

The data listed in Table 2 show that the ***trans*-I** rotamer is the most stable and the trans forms present lower energies than the cis ones, although small relative differences. A thorough analysis about the responsible effects by conformational stabilities will be given in sequence.

NMR data and IR spectra can now be used to determine the conformational preferences on ProOMe and AcProOMe, in solution. The use of these spectroscopies in conformational analysis is very well established and has provided reliable results.[12,13,32−36] According to Karplus[37] it is known that the $^3J_{HH}$ coupling constant is dependent on the dihedral angles between

dx.doi.org/10.1021/jp5007632 | J. Phys. Chem. A 2014, 118, 1748−1758

Table 2. Calculated Structural Parameters,[a] Energies (E),[b] and Dipole Moments (μ) for the Optimized Conformer Structures of AcProOMe in Isolated Phase, at the ωB97X-D/aug-cc-pVTZ Level of Theory

parameter	*trans*-I	*trans*-II	*cis*-I	*cis*-II
r(N−C_3)	1.451	1.447	1.443	1.446
r(N−C_{20})	1.357	1.358	1.360	1.359
r(C_3−C_9)	1.521	1.524	1.526	1.526
ω[O═C−O−C]	2.6	2.9	1.2	0.3
ψ[N−C−C═O]	39.7	164.6	18.4	161.7
θ[C−C(═O)−N−C]	177.4	179.2	0.8	1.4
E (au)	−592.95471	−592.95455	−592.95425	−592.95408
E_{rel} (kcal mol^{-1})[c]	0.00	0.10	0.28	0.39
μ (debye)	3.74	5.25	5.51	2.80
population (%)	31.9	31.9	19.8	16.4

[a]Bond lengths in angstroms (Å); bond and dihedral angles in degrees. [b]ZPE correction included. [c]1 au = 627.5095 kcal mol^{-1}.

Table 3. Experimental Chemical Shifts (ppm) and Vicinal Spin−Spin Coupling Constants (Hz) Obtained in Solvents of Different Dielectric Constants (ε) for the ProOMe

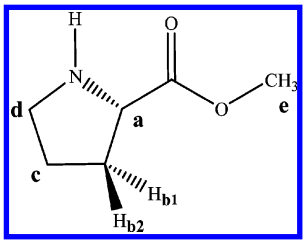

solvent	ε	δH_a	δH_{b1}	δH_{b2}	δH_c	δH_{d1}	δH_{d2}	δH_e	$^3J_{HaHb1}$	$^3J_{HaHb2}$
pyridine-d_5	12.4	3.89	2.00	1.83	1.61	3.07	2.89	3.62	5.9	8.5
acetone-d_6	20.7	4.18	2.29	1.82	1.94	3.25	3.16	3.78	5.9	9.2
CD_3CN	37.5	4.06	2.24	1.79	1.90	3.21	3.06	3.77	6.2	9.1
DMSO-d_6	46.7	3.78	2.06	1.75	1.70	2.99	2.84	3.66	6.0	8.7

these atoms, providing information about the spacial orientation. Furthermore, in an equilibrium where the interconversion rate between the conformers is very fast, the observed $^3J_{HH}$ coupling constant in the NMR spectra corresponds to a weighted mean due to the contribution of each conformer, as shown by the following equation:

$$^3J_{HH} = \sum n_i/n_t\, ^3J_i \quad (1)$$

where n_i/n_t is the relative population of each conformer i and ^3J_i is the individual coupling constant. As $^3J_{HH}$ is dependent on the conformer populations, and these populations can be affected by the solvent, the conformational behavior of ProOMe and AcProOMe conformers may be evaluated through the $^3J_{HH}$.[38] Thus, the ^{1}H NMR spectra were obtained in solvents of several polarities. However, according to data in Table 3 the $^3J_{HH}$ values for ProOMe showed no significant changes (between 5.9 in pyridine-d_5 and 6.2 in CD_3CN for $^3J_{HaHb1}$ and between 8.5 in pyridine-d_5 and 9.2 in acetone-d_6 for $^3J_{HaHb2}$), indicating variations that do not occur in the conformer populations in the equilibria. Moreover, relating the conformer H_a−C−C−H_{b1} dihedral angles (approximately 135° for **I** and 92° for **II**) and H_a−C−C−H_{b2} (15° for **I** and 26° for **II**) with the Karplus curve[39] and comparing with the experimental $^3J_{HH}$, these results suggest a greater proximity to conformer **I** geometry, indicating its higher proportion. It should be taken into account that the measured couplings are related to the proline ring, and the conformational changes involve side chain. However, it was noted that on changing N−C−C═O dihedral angle (theoretical calculations), significant variations in the H_a−C−C−H_{b1} dihedral angle were observed. Thus, both changes are intimately related.

For AcProOMe, each ^{1}H NMR spectrum obtained at room temperature showed signals due to both cis and trans rotamers about the *N*-COMe bond since the interconversion of the two isomers is slow on the NMR time scale, with a barrier sufficiently large (approximately 22.5 kcal/mol, obtained from theoretical calculations at the B3LYP/cc-pVDZ level of theory) between both forms. Nevertheless, like ProOMe, the $^3J_{HH}$ values for AcProOMe (Table 4) remained almost unchanged in different solvents.

Table 4. Vicinal Spin−Spin Coupling Constants (Hz) Obtained in Solvents of Different Dielectric Constants (ε) for the AcProOMe

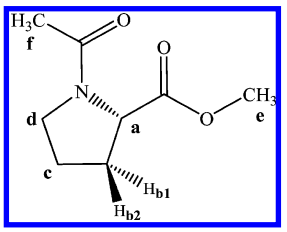

		cis		trans	
solvent	ε	$^3J_{HaHb1}$	$^3J_{HaHb2}$	$^3J_{HaHb1}$	$^3J_{HaHb2}$
C_6D_6	2.3	2.7	8.5	3.9	
$CDCl_3$	4.8	2.7	8.7	3.9	8.7
CD_2Cl_2	9.10	2.8		3.9	8.8
pyridine-d_5	12.4	2.7	8.6	3.8	8.7
acetone-d_6	20.7	2.6	8.7	4.1	8.7
CD_3CN	37.5	2.6	8.7	4.4	8.7
DMSO-d_6	46.7	2.6	8.7	4.3	8.7

dx.doi.org/10.1021/jp5007632 | J. Phys. Chem. A 2014, 118, 1748−1758

On the basis of the integration of peaks in the ^{1}H NMR spectra, it was verified that, in all the solvents, the trans rotamer is in great excess (about 80%) compared to the *cis*. Moreover, by associating the $H_a-C-C-H_{b1}$ dihedral angles of ***trans*-I** (145°) and ***trans*-II** (86°) conformers and the Karplus relation with the $^3J_{HaHb1}$ coupling constant obtained for *trans* form (approximately 4.0 Hz), it is noted that the latter results from the contribution of these two conformers. In turn, these relationships can not be used to determine the lowest energy conformer of the cis form since the ***cis*-I** and ***cis*-II** conformers have almost equal values of this angle. With respect to $H_a-C-C-H_{b2}$ dihedral angles of the four conformers, their angles are approximately 30°, and therefore, their experimental $^3J_{HaHb2}$ coupling constants are very similar (ca. 8.7 Hz).

The solvent influence on the conformer stabilities was evaluated by theoretical calculations with the IEF-PCM (Table 5) in order to understand the conformational preferences of the compounds and to compare the experimental data with the theoretical values. Additionally, the $^3J_{HaHb}$ coupling constants were calculated for each conformer of ProOMe and AcProOMe in the solvents where $^3J_{HaHb}$ values were experimentally measured and are portrayed in Figures 5a,b and 6a,b, respectively. Comparison of the conformer populations indicated that they remain pratically unaffected by changing the solvent, and the calculated $^3J_{HaHb}$ values are in accordance with the experimental data. Furthermore, in all solvents examined, the conformers **I** and ***trans*-I** are the most stable, corresponding to populations of about 90% and 43% in the conformational equilibria of ProOMe and AcProOMe, respectively.

Table 5. Populations in Solution for the ProOMe and AcProOMe Conformers Using the IEF-PCM Solvation Model, Calculated at the ωB97X-D/aug-cc-pVTZ Level of Theory

	ProOMe		AcProOMe			
	I	**II**	***trans*-I**	***trans*-II**	***cis*-I**	***cis*-II**
CCl_4	92.9	7.1	40.8	29.6	15.8	13.8
$CHCl_3$	91.7	8.3	42.3	29.2	16.4	12.1
CH_2Cl_2	90.6	9.4	43.6	29.5	16.4	10.5
pyridine	89.4	10.6	43.7	30.0	16.4	9.9
acetone	89.4	10.6	43.9	30.8	16.2	9.1
CH_3CN	88.9	11.1	43.9	31.3	16.1	8.7
DMSO	88.7	11.3	43.7	31.7	16.1	8.5

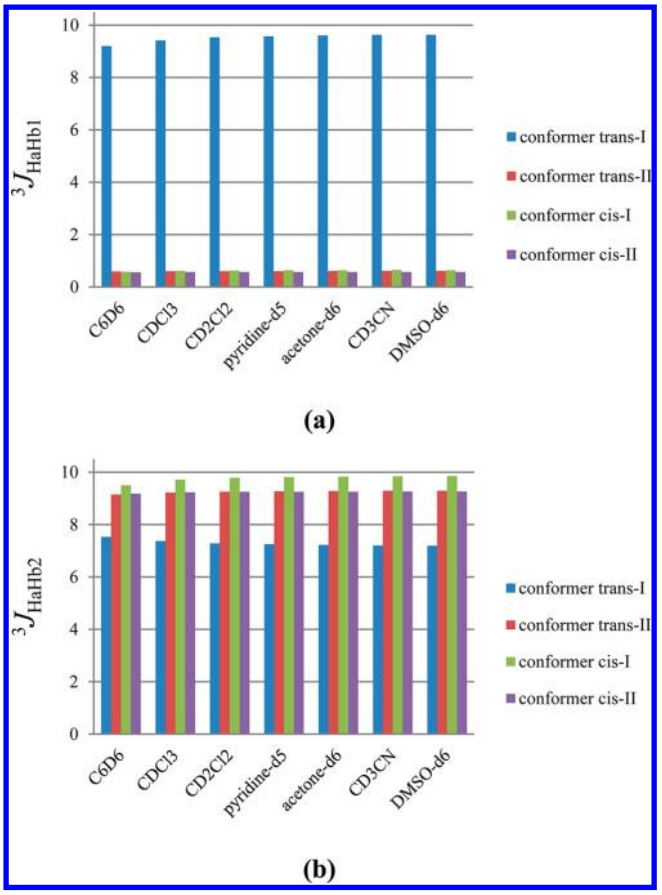

Figure 6. Spin−spin coupling constants (a) $^3J_{HaHb1}$ and (b) $^3J_{HaHb2}$ calculated for each conformer of AcProOMe at the ωB97X-D/EPR-III, by using the IEFPCM in solvents of different dielectric constants.

By comparing the values experimentally obtained for ProOMe (Table 3) with the calculated values (Figure 5a,b), it can be noted that the experimental $^3J_{HaHb1}$ values (about 6.0 Hz) show more similarity to the conformer **I**, whose mean value in different solvents is 7.7 Hz, whereas for the conformer **II** it is 3.1 Hz. This result again confirms that **I** is the most stable conformation in the equilibrium of this compound. Similarly for AcProOMe, the calculated $^3J_{HaHb1}$ values in all the solvents of ***trans*-I** and ***trans*-II** (Figure 6a,b) have quite different values (approximately 9.4 and 0.5 Hz, respectively). Therefore, as these conformers present

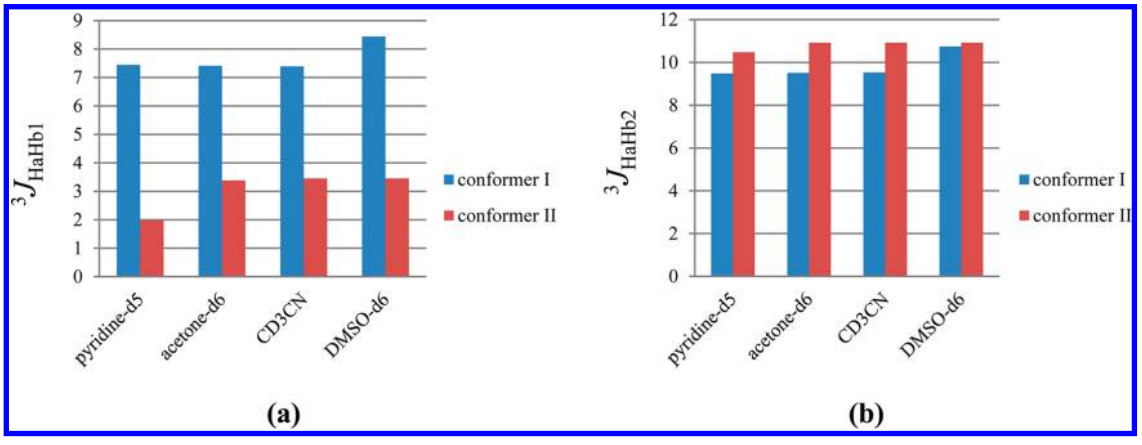

Figure 5. Spin−spin coupling constants (a) $^3J_{HaHb1}$ and (b) $^3J_{HaHb2}$ calculated for each conformer of ProOMe at the ωB97X-D/EPR-III, by using the IEFPCM in solvents of different dielectric constants.

dx.doi.org/10.1021/jp5007632 | J. Phys. Chem. A 2014, 118, 1748−1758

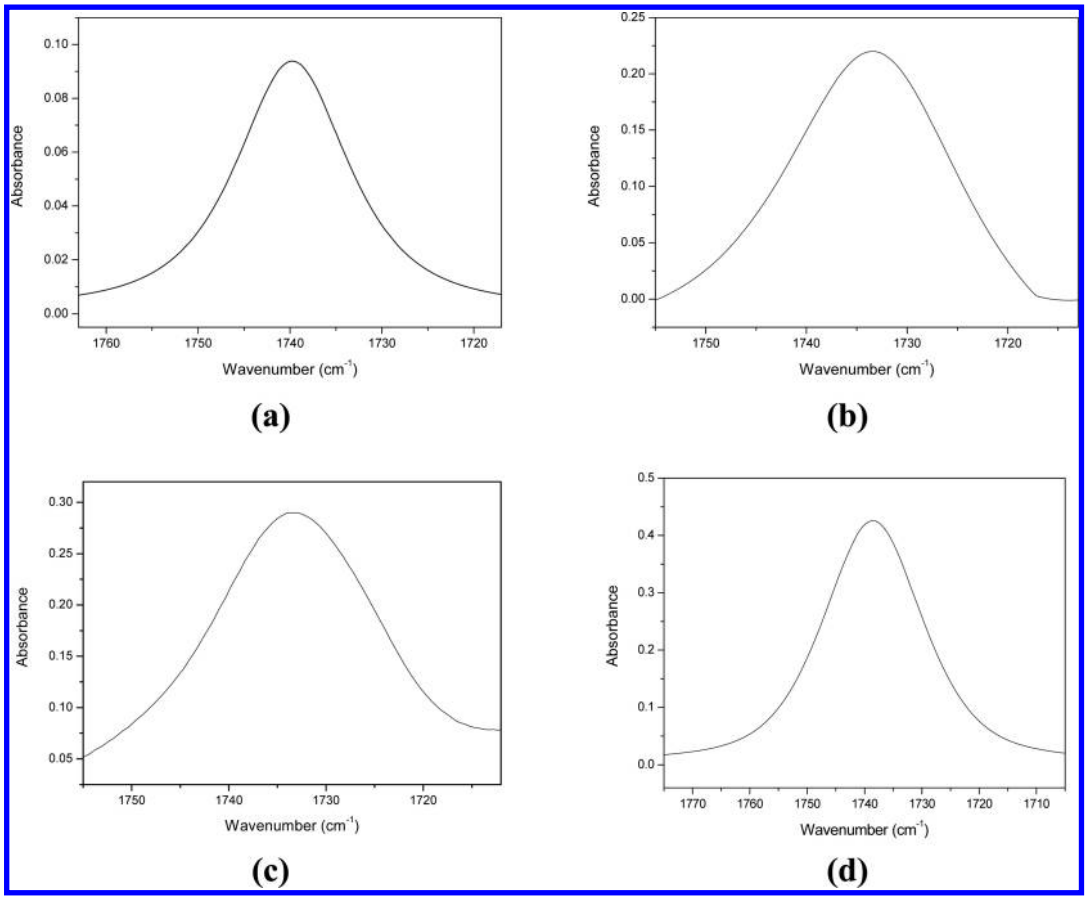

Figure 7. IR spectra of ProOMe showing the carbonyl absorption bands in (a) CCl_4, (b) $CHCl_3$, (c) CH_2Cl_2, and (d) CH_3CN, in the fundamental region.

Table 6. Experimental and Calculated Wavenumbers (ν, in cm^{-1}) and Intensities (P, in %) of the Ester Carbonyl Stretching Bands in the IR Spectra of AcProOMe; Theoretical Data in Solution Were Obtained through the IEF-PCM-ωB97X-D/aug-cc-pVTZ Level of Theory

	CCl_4						$CHCl_3$					
	exptl		theor				exptl		theor			
group[a]	ν	P	ν[b]	E_{rel}[c]	P	P_T	ν	P	ν	E_{rel}	P	P_T
I	1754.2	52.5	1823.3	0.00	35.4	52.0	1747.7	57.3	1813.1	0.00	42.3	58.7
			1825.8	0.45	16.6				1814.6	0.56	16.4	
II	1745.3	47.5	1815.9	0.02	34.3	48.0	1736.2	42.7	1805.3	0.22	29.2	41.3
			1811.9	0.56	13.7				1801.7	0.74	12.1	
	CH_2Cl_2						CH_3CN					
	exptl		theor				exptl		theor			
group	ν	P	ν	E_{rel}	P	P_T	ν	P	ν	E_{rel}	P	P_T
I	1749.0	60.1	1807.1	0.00	43.6	60.0	1750.1	62.8	1800.7	0.00	43.9	60.1
			1808.2	0.58	16.4				1801.4	0.59	16.2	
II	1737.7	39.9	1798.1	0.23	29.5	40.0	1738.3	37.2	1790.5	0.20	31.3	39.9
			1796.3	0.84	10.5				1791.0	0.96	8.6	

[a]Group I included ***trans*-I** and ***cis*-I** conformers, and the group II is composed by ***trans*-II** and ***cis*-II** conformers. [b]Calculated wavenumber values are overestimated regarding the experimental values due to anharmonicity effects; however, the relationship among the wavenumbers of the conformers do not change. [c]Relative energies in kcal mol^{-1}.

similar stabilities, it can be explained that the value of this experimental coupling constant (~4.0 Hz) for the trans form is a result of averaging of these conformations. In contrast, the $^3J_{HaHb2}$ has values very close for all the geometries and may not be used for such argument.

Besides NMR, the IR spectra have been well accepted to estimate the behavior of conformer populations with variation of the solvent.[32−36] The C═O stretching band is appropriate for this type of analysis since it has a strong absorption in a relatively clear region of the IR spectrum. So, the analysis of the ProOMe carbonyl stretching band in different solvents (CCl_4, $CHCl_3$, CH_2Cl_2, and CH_3CN) (Figure 7) revealed the presence of a single symmetrical band supporting the earlier conclusions of the occurrence of a major conformer in solution and that the

dx.doi.org/10.1021/jp5007632 | J. Phys. Chem. A 2014, 118, 1748−1758

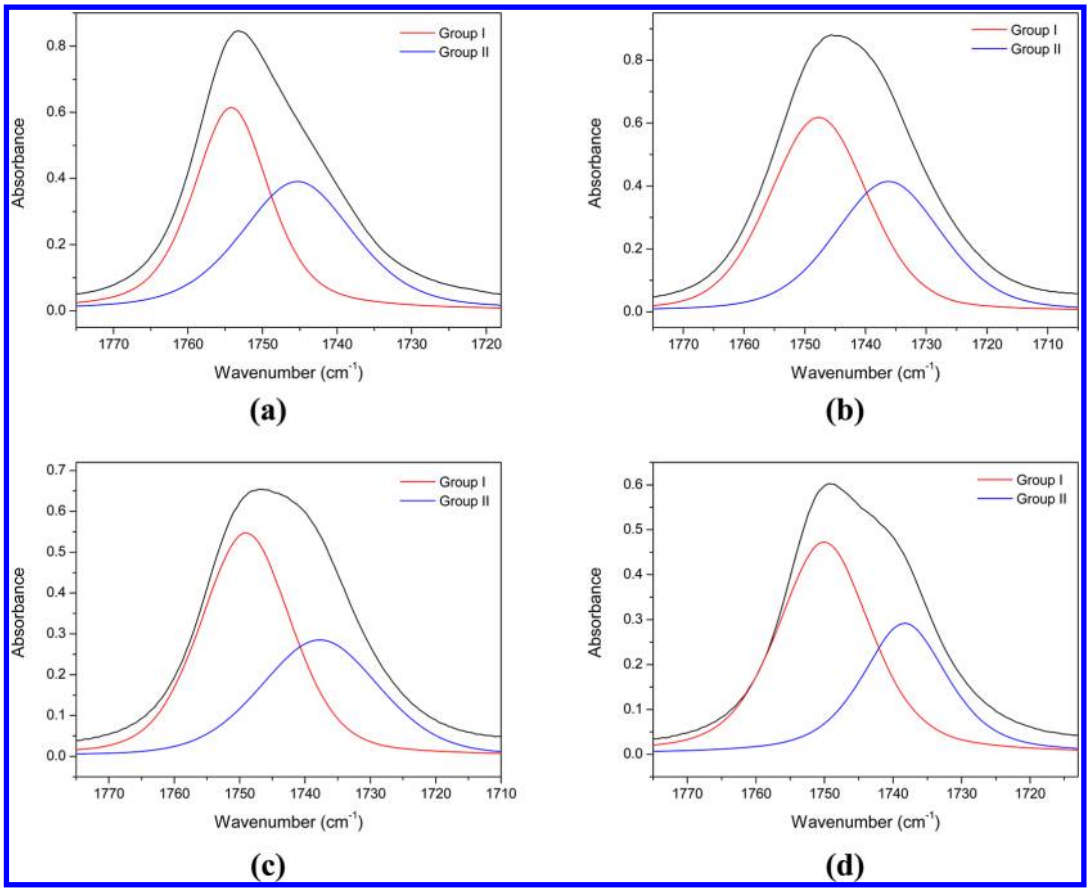

Figure 8. IR spectra of AcProOMe showing the carbonyl absorption band in (a) CCl_4, (b) $CHCl_3$, (c) CH_2Cl_2, and (d) CH_3CN, in the fundamental region. Groups **I** and **II** are described in Table 6.

Table 7. Main Orbital Interactions and Corresponding Energies (in kcal mol^{-1}) for Conformers of ProOMe and AcProOMe Calculated at the ωB97X-D/aug-cc-pVTZ Level

	ProOMe		AcProOMe			
orbital interaction	**I**	**II**	***trans*-I**	***trans*-II**	***cis*-I**	***cis*-II**
$n_{N(1)} \rightarrow \pi^*_{C20=O25}$			91.03	91.89	90.00	89.74
$n_{O15(2)} \rightarrow \pi^*_{C9=O14}$	68.22	59.11	70.94	68.79	68.59	69.44
$n_{O14(2)} \rightarrow \sigma^*_{C9-O15}$	41.17	42.76	41.58	42.38	41.99	42.20
$n_{O25(2)} \rightarrow \sigma^*_{N-C20}$			29.82	30.43	30.99	30.83
$n_{O14(2)} \rightarrow \sigma^*_{C3-C9}$	24.56	24.19	26.28	24.53	26.83	24.51
$n_{O25(2)} \rightarrow \sigma^*_{C20-C21}$			25.30	25.45	25.41	25.35
$n_{O15(1)} \rightarrow \sigma^*_{C9=O14}$	10.28	9.46	10.71	10.07	10.40	10.29
$n_{N(1)} \rightarrow \sigma^*_{C3-C9}$	6.75	12.15	8.06	11.15	11.98	12.45

conformational equilibrium of ProOMe is not affected by solvent.

The AcProOMe IR spectra analysis was carried out using the ester carbonyl group because according to the calculated frequencies this stretching band presents larger differences among the conformers than the amide one. Furthermore, it is necessary that the carbonyl frequencies of each conformer are sufficiently different in order that the corresponding bands, even if superimposed, can be computationally resolved by deconvolution. In this sense, on the basis of this ester C═O stretching predicted by theoretical calculations, the four conformers were divided in two groups, each one with one cis and one trans form presenting the same pyrrolidine ring arrangement.

Table 6 gives the infrared spectral data and also the theoretically calculated values at the IEFPCM-ωB97X-D/aug-cc-pVTZ level, and Figure 8 shows the deconvolution of the ester carbonyl band. According to the calculated energies and NMR data, it is evident that the *trans* conformers predominate in the equilibrium in relation to the cis, by a ratio of approximatelly 70:30, considering the same ring arrangement. This behavior leads to the assignment of trans rotamers as the major contributors of each band component determined by deconvolution. On the basis of this assumption, the good agreement between the experimental results (by NMR and IR spectroscopies) and the theoretical ones, highlighting the higher stability of the trans in comparison with cis conformers, and that the solvents do not affect the relative energies of AcProOMe conformers is remarkable.

NBO calculations were performed in order to get a detailed insight into the effects that rule the preference for the most stable conformers. The main orbital interactions presented in Table 7

dx.doi.org/10.1021/jp5007632 | J. Phys. Chem. A 2014, 118, 1748−1758

and shown in Figures S1 and S2 (Supporting Information) were used to interpret their stability in terms of hyperconjugative effects. The data indicated that all the conformers are mainly stabilized by interactions involving the nitrogen and oxygen nonbonding electron pairs as donors. The most important interaction that takes place in ProOMe is the $n_{O15(2)} \rightarrow \pi^*_{C9=O14}$, which is approximately 9.0 kcal mol^{-1} more energetic for conformer **I** in relation to conformer **II**, and it is mainly responsible for the higher stability of the former. This hyperconjugation is also observed in AcProOMe, its second most energetic, only after the $n_{N(1)} \rightarrow \pi^*_{C20=O25}$. There are also another two interactions with high energies for ProOMe: $n_{O14(2)} \rightarrow \sigma^*_{C9-O15}$ and $n_{O14(2)} \rightarrow \sigma^*_{C3-C9}$, and apart from these, $n_{O25(2)} \rightarrow \sigma^*_{N-C20}$ and $n_{O25(2)} \rightarrow \sigma^*_{C20-C21}$, for AcProOMe, which are similar for all conformations.

Additionally, NBO analysis, QTAIM method, and geometrical parameters were employed to characterize a possible O···H−N intramolecular hydrogen bonding (IHB) in ProOMe. According to NBO calculations, conformer **I** is the only one that shows a $n_O \rightarrow \sigma^*_{N-H}$ hyperconjugative interaction. Although this interaction gives an additional stability for this conformation concerning **II**, it has a value of 0.51 kcal mol^{-1}, which is very weak and does not characterize an IHB. Indeed, an analysis of the QTAIM molecular graphs (Figure S3, Supporting Information) and the parameters r(NH···O) and ∠NH···O (Table 1) indicate that both conformers did not form an IHB.[40,41] The main reason for its nonoccurrence is due to geometrical restrictions caused by the presence of the pyrrolidine ring.

In the case of AcProOMe, despite the ***trans*-I** isomer presenting a high steric repulsion due to repelling lone pairs of the oxygen atoms, which are directed toward each other, a $n_{O25(2)} \rightarrow \pi^*_{C9-O14}$ stabilizing interaction of 1.71 kcal mol^{-1} larger in relation to the same interaction in the ***trans*-II** conformer contributes to its conformational preference (Figure 9).

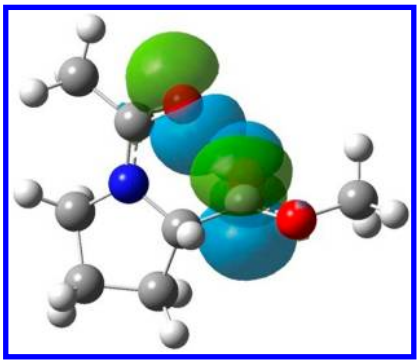

Figure 9. Orbital overlap of the $n_{O25(2)} \rightarrow \pi^*_{C9-O14}$ interaction that stabilizes the conformer ***trans*-I** of AcProOMe.

In order to evaluate the role of the hyperconjugative and steric effects in the conformer stabilities, NBO calculations were carried out with deletion of all hyperconjugations. The NBO analysis generates structures with localized orbitals, in other words, an idealized Lewis structure, where bonding orbitals and lone pairs are doubly occupied. However, this analysis also produces antibonding (σ^* and π^*), which may lead to hyperconjugative interactions. Thus, the deletion of all antibonding and Rydberg orbitals results in strictly localized Lewis structures, in which only classic interactions (steric and electrostatic) are present, making possible the determination the steric and hyperconjugative contributions. Then, the energies before (ΔE_{full}) and after the removal of hyperconjugative contributions (ΔE_{Lewis}) are obtained. The differences in energy between the conformers are shown in Table 8 and reveal that for both compounds, although

Table 8. Total Conformational Energies (ΔE_{full}),[a] Steric (ΔE_{Lewis}), and Hyperconjugative (ΔE_{hyper}) Contributions to the ΔE_{full} Values of ProOMe and AcProOMe Conformers (in kcal mol^{-1}), at the ωB97X-D/aug-cc-pVTZ Level

	ProOMe		AcProOMe			
	I	**II**	***trans*-I**	***trans*-II**	***cis*-I**	***cis*-II**
ΔE_{full}	0.00	1.78	0.00	0.20	0.36	0.57
ΔE_{Lewis}	3.82	0.00	6.92	0.00	4.17	5.67
ΔE_{hyper}	5.60	0.00	7.12	0.00	4.02	1.28

[a] $\Delta E_{full} = \Delta E_{Lewis} + \Delta E_{hyper}$.

the most stable conformers (**I** and ***trans*-I**, for ProOMe and AcProOMe, respectively) present the highest destabilizing character associated with the steric factor (greater ΔE_{Lewis}), the stabilizing effect, provided by hyperconjugation (higher ΔE_{hyper}), compensates that desestabilization and explains their greater predominance in the equilibria. Furthermore, for the other conformers of AcProOMe, the lower energies (ΔE_{full}) are associated with the smaller steric effects.

Therefore, the results for AcProOMe suggest that the interplay between hyperconjugation and steric hindrance rules its rotational isomerism. In this way, a higher contribution of steric effects in AcProOMe, in comparison to ProOMe, should be due to the perturbation caused by the *N*-acetyl group.

4. CONCLUSIONS

Since the experimental study of amino acids conformational equilibrium is difficult for the several reasons discussed in this work, it was performed through the substitution of an acidic group by the corresponding methyl ester, which is soluble in organic solvents, does not show a zwitterionic form in solution, and presents a conformational behavior similar to that of amino acids. The experimental results obtained through ^{1}H NMR and IR spectroscopies demonstrated that the ProOMe and AcProOMe equilibra do not exhibit solvent effects and are in agreement with the theoretical calculations, which provide an insight into their conformational behavior. ProOMe showed the existence of one conformer with a population of about 90%, both in isolated phase and solution, whereas for AcProOMe the trans rotamers predominate compared to the cis.

The conformer stabilities were explained by NBO analysis, which showed that the occurrence of hyperconjugative interactions plays a determinant role to stabilize the lower energy conformer of ProOMe, predominating over its larger steric effect. However, for AcProOMe an interplay between stereoelectronic and steric effects underlies molecular conformation.

Thus, the information provided by this work allows a better understanding of conformational behavior of amino acids in solution and may be extended to more complex systems, such as peptides and proteins.

■ ASSOCIATED CONTENT

Supporting Information

Natural bond orbitals illustrating the main hyperconjugative interactions that stabilize the lower energy conformers of the analyzed compounds; molecular graphs for conformers of ProOMe. This material is available free of charge via the Internet at http://pubs.acs.org.

dx.doi.org/10.1021/jp5007632 | J. Phys. Chem. A 2014, 118, 1748−1758

AUTHOR INFORMATION

Corresponding Author

*(R.R.) E-mail: rittner@iqm.unicamp.br. Tel: +55-19-3521-3150.

Notes

The authors declare no competing financial interest.

ACKNOWLEDGMENTS

The authors thank a grant #2012/03933-5 from São Paulo Research Foundation (FAPESP) for financial support of this work and for a scholarship (to C.B.B. #2012/18567-4). Thanks also go to Conselho Nacional de Pesquisa (CNPQ) for the fellowships (to R.R. and C.F.T).

REFERENCES

(1) Gronert, S.; O'Hair, R. A. J. Ab Initio Studies of Amino Acid Conformations. 1. The Conformers of Alanine, Serine, and Cysteine. *J. Am. Chem. Soc.* **1995**, *117*, 2071−2081.

(2) Lessari, A.; Mata, S.; Cocinero, E. J.; Blanco, S.; López, J. C.; Alonso, J. L. The Structure of Neutral Proline. *Angew. Chem., Int. Ed.* **2002**, *41*, 4673−4676.

(3) Jaeger, H. M.; Schaefer, H. F., III; Demaison, J.; Császar, A. G.; Allen, W. D. Lowest-Lying Conformers of Alanine: Pushing Theory to Ascertain Precise Energetics and Semiexperimental R_e Structures. *J. Chem. Theory Comput.* **2010**, *6*, 3066−3078.

(4) Kapitán, J.; Baumruk, V.; Kopecky, V.; Pohl, R.; Bour, P. Proline Zwitterion Dynamics in Solution, Glass, and Crystalline State. *J. Am. Chem. Soc.* **2006**, *128*, 13451−13462.

(5) Schmidt, J.; Kass, S. R. Zwitterion vs Neutral Structures of Amino Acids Stabilized by a Negatively Charged Site: Infrared Photodissociation and Computations of Proline−Chloride Anion. *J. Phys. Chem. A* **2013**, *117*, 4863−4869.

(6) Lessari, A.; Cocinero, E. J.; López, J. C.; Alonso, J. L. The Shape of Neutral Valine. *Angew. Chem., Int. Ed.* **2004**, *43*, 605−610.

(7) Lessari, A.; Sanchéz, R.; Cocinero, E. J.; López, J. C.; Alonso, J. L. Coded Amino Acids in Gas Phase: The Shape of Isoleucine. *J. Am. Chem. Soc.* **2005**, *127*, 12952−12956.

(8) Alonso, J. L.; Cocinero, E. J.; Lessari, A.; Sanz, M. E.; López, J. C. The Glycine−Water Complex. *Angew. Chem., Int. Ed.* **2006**, *45*, 3471−3474.

(9) Blanco, S.; Sanz, M. E.; López, J. C.; Alonso, J. L. Revealing the Multiple Structures of Serine. *Proc. Natl. Acad. Sci.* **2007**, *104*, 20183−20188.

(10) Cocinero, E. J.; Villanueva, P.; Lessari, A.; Sanz, M. E.; Blanco, S.; Mata, S.; López, J. C.; Alonso, J. L. The Shape of Neutral Sarcosine in Gas Phase. *Chem. Phys. Lett.* **2007**, *435*, 336−341.

(11) Alonso, J. L.; Pérez, C.; Sanz, M. E.; López, J. C. Seven Conformers of L-Htreonine in the Gas Phase: a LA-MB-FTMW Study. *Phys. Chem. Chem. Phys.* **2009**, *11*, 617−627.

(12) Cormanich, R. A.; Ducati, L. C.; Tormena, C. F.; Rittner, R. A Theoretical and Experimental ^{1}H NMR Spectroscopy Study of the Stereoelectronic Interactions That Rule the Conformational Energies of Alanine and Valine Methyl Ester. *J. Phys. Org. Chem.* **2013**, *26*, 849−857.

(13) Duarte, C. J.; Cormanich, R. A.; Ducati, L. C.; Rittner, R. ^{1}H NMR and Theoretical Studies on the Conformational Equilibrium of Tryptophan Methyl Ester. *J. Mol. Struct.* **2013**, *1050*, 174−179.

(14) Deber, C. M.; Brodsky, B.; Rath, A. Proline Residues in Proteins. In *Encyclopedia of Life Sciences*; John Wiley & Sons: Chichester, U.K., 2010; pp 1−9.

(15) Stepanian, S. G.; Reva, I. D.; Radchenko, E. D.; Adamowicz, L. Conformers of Nonionized Proline. Matrix-Isolation Infrared and Post-Hartree-Fock ab Initio Study. *J. Phys. Chem. A* **2001**, *105*, 10664−10672.

(16) Haasnoot, C. A. G.; Leeuw, F. A. A. M.; Leeuw, H. P. M.; Altona, C. Relationship Between Proton−Proton NMR Coupling Constants and Substituent Electronegativities. III. Conformational Analysis of Proline Rings in Solution Using a Generalized Karplus Equation. *Biopolymers* **1981**, *20*, 1211−1245.

(17) Aliev, A. E.; Courtier-Murias, D. Conformational Analysis of L-Prolines in Water. *J. Phys. Chem. B* **2007**, *111*, 14034−14042.

(18) Aliev, A. E.; Bhandal, S.; Courtier-Murias, D. Quantum Mechanical and NMR Studies of Ring Puckering and *cis/trans*-Rotameric Interconversion in Prolines and Hydroxyprolines. *J. Phys. Chem. A* **2009**, *113*, 10858−10865.

(19) Cormanich, R. A.; Ducati, L. C.; Tormena, C. F.; Rittner, R. A Theoretical Investigation of the Dictating Forces in Small Amino Acid Conformational Preferences: The Case of Glycine, Sarcosine and *N,N*-Dimethylglycine. *Chem. Phys.* **2013**, *421*, 32−38.

(20) Cormanich, R. A.; Ducati, L. C.; Rittner, R. The Lack of Intramolecular Hydrogen Bonding and the Side Chain Effect in Alanine Conformers. *J. Mol. Struct.* **2012**, *1014*, 12−16.

(21) Cormanich, R. A.; Ducati, L. C.; Rittner, R. Are Hydrogen Bonds Responsible for Glycine Conformational Preferences? *Chem. Phys.* **2011**, *387*, 85−91.

(22) Ananda, K.; Babu, V. V. S. Deprotonation of Hydrochloride Salts of Amino Acid Esters and Peptide Esters Using Commercial Zinc Dust. *J. Peptide Res.* **2001**, *57*, 223−226.

(23) Uhle, F. C.; Harris, L. S. The Synthesis of α-Methylamino Acids. *J. Am. Chem. Soc.* **1956**, *78*, 381−384.

(24) Yamada, T.; Lukac, P. J.; Yu, T.; Weiss, R. G. Reversible, Room-Temperature, Chiral Ionic Liquids. Amidinium Carbamates Derived from Amidines and Amino-Acid Esters with Carbon Dioxide. *Chem. Mater.* **2007**, *19*, 4761−4768.

(25) *GRAMS/AI*, version 9.0; ThermoFisher: Wobum, MA, 2009.

(26) Chai, J.-D.; Head-Gordon, M. Long-Range Corrected Hybrid Density Functionals with Damped Atom−Atom Dispersion Corrections. *Phys. Chem. Chem. Phys.* **2008**, *10*, 6615−6620.

(27) Cancès, E.; Mennucci, B.; Tomasi, J. A New Integral Equation Formalism for the Polarizable Continuum Model: Theoretical Background and Applications to Isotropic and Anisotropic Dielectrics. *J. Chem. Phys.* **1997**, *107*, 3032−3041.

(28) Frisch, M. J.; Trucks, G. W.; Schlegel, H. B.; Scuseria, G. E.; Robb, M. A.; Cheeseman, J. R.; Scalmani, G.; Barone, V.; Mennucci, B.; Petersson, G. A.; et al. *Gaussian 09*, revision B.01; Gaussian, Inc.: Wallingford, CT, 2010.

(29) *NBO*, version 5.0, implemented in the Gaussian 09 package of programs; Gaussian Inc: Wallingford, CT, 2009.

(30) Keith, T. A. *AIMALL* (version 11.12.19); TK Gristmill Software: Overland Park, KS, 2011; aim.tkgristmill.com.

(31) Reddy, D. N.; Thirupathi, R.; Tumminakatti, S.; Prabhakaran, E. N. A Method for Stabilizing the *cis* Prolyl Peptide Bond: Influence of an Unusual $n \rightarrow \pi^*$ Interaction in 1,3-Oxazine and 1,3-Thiazine Containing Peptidomimetics. *Tetrahedron Lett.* **2012**, *53*, 4413−4417.

(32) Rittner, R.; Ducati, L. C.; Tormena, C. F.; Fiorin, B. C.; Braga, C. B. Conformational Preferences for Some 5-Substituted 2-Acetylthiophenes through Infrared Spectroscopy and Theoretical Calculations. *Spectrochim. Acta, Part A* **2011**, *79*, 1071−1076.

(33) Rittner, R.; Ducati, L. C.; Tormena, C. F.; Fiorin, B. C.; Braga, C. B.; Abraham, R. J. Studies on the *s-cis−trans* Isomerism for Some Furan Derivatives through IR and NMR Spectroscopies and Theoretical Calculations. *Spectrochim. Acta, Part A* **2013**, *103*, 84−89.

(34) Ducati, L. C.; Braga, C. B.; Rittner, R.; Tormena, C. F. A Critical Evaluation of the *s-cis−trans* Isomerism of 2-Acetylpyrrole and Its *N*-Methyl Derivative through Infrared and NMR Spectroscopies and Theoretical Calculations. *Spectrochim. Acta, Part A* **2013**, *116*, 196−203.

(35) Rozada, T. C.; Gauze, G. F.; Favaro, D. C.; Rittner, R.; Basso, E. A. Infrared and Theoretical Calculations in 2-Halocycloheptanones Conformational Analysis. *Spectrochim. Acta, Part A* **2012**, *94*, 277−287.

(36) Melo, U. Z.; Gauze, G. F.; Bagatin, M. C.; Pontes, R. M.; Basso, E. A. A Theoretical and Experimental Study of the Conformational Behavior of *trans*-2-Azidocyclohexanol in Solution. *J. Mol. Struct.* **2012**, *1026*, 93−101.

(37) Karplus, M. Contact Electron-Spin Coupling of Nuclear Magnetic Moments. *J. Chem. Phys.* **1959**, *30*, 11−15.

(38) Hore, P. J. *Nuclear Magnetic Resonance*; Oxford University Press: New York, 1995.

(39) Karplus, M. Vicinal Proton Coupling in Nuclear Magnetic Resonance. *J. Am. Chem. Soc.* **1963**, *85*, 2870−2871.
(40) Grabowski, S. J. What Is the Covalency of Hydrogen Bonding? *Chem. Rev.* **2011**, *111*, 2597−2625.
(41) Koch, U.; Popelier, P. L. A. Characterization of C−H−O Hydrogen Bonds on the Basis of the Charge Density. *J. Phys. Chem.* **1995**, *99*, 9747−9754.